Open Access

OBM Neurobiology

Research Article

Magnetic Resonance Imaging Approaches for Predicting the Response to Hyperoxic Radiotherapy in Glioma-Bearing Rats

Nuria Arias-Ramos [1, †], Jesús Pacheco-Torres [1, 2, †], Pilar López-Larrubia [1, *]

1. Instituto de Investigaciones Biomédicas "Alberto Sols", CSIC-UAM, Madrid, Spain; E-mails: narias@iib.uam.es; pachecotorres@gmail.com; plopez@iib.uam.es
2. Division of Cancer Imaging Research, The Russell H. Morgan Department of Radiology and Radiological Science, The Johns Hopkins University School of Medicine, Baltimore, MD, USA

† These authors contributed equally to this work.

* **Correspondence:** Pilar López-Larrubia; E-mail: plopez@iib.uam.es

Academic Editor: Antonio Meola

Special Issue: Tumors of the Central Nervous System

OBM Neurobiology
2019, volume 3, issue 1
doi:10.21926/obm.neurobiol.1901020

Received: November 11, 2018
Accepted: January 28, 2019
Published: January 31, 2019

Abstract

***Background*:** Despite important advances in multimodal therapeutic options, glioblastoma (GBM), the most frequent and aggressive form of all astrocytomas, remains with a median overall survival period of 15 months. A direct correlation between GBM hypoxia and higher aggressiveness, poor prognosis and greater resistance to different treatments has been established. However, because of intratumoral and interindividual heterogeneity, it has not been possible to assess accurately the hypoxia degree from physiopathological parameters or neuroimaging methods. This study aims to develop and evaluate a magnetic resonance imaging (MRI) approach to identify more precisely those tumors that could improve the outcome through an oxygen targeted therapy.

***Methods*:** To assess the efficacy of radiotherapy in animals irradiated under air and oxygen breathing, we implemented a GBM animal model obtained by intracranial injection of glioma C6 cells in rats. MRI studies, based on the oxygen-induced contrast in blood (BOLD) and

tissues (TOLD), were carried out to evaluate the effect of the modulation in oxygen breathing conditions on the tumors *in vivo*. The efficacy of the oxygen breathing therapies was determined by the relative tumor volume at the end of the experiment, compared to its size on the day before the treatment.

***Results*:** Our results categorized the tumors in responding, non-responding and intermediate behaviors. While BOLD analysis did not show any statistical difference between animals, either breathing air or oxygen, TOLD parameters allowed for the identification of the tumors with higher responses to hyperoxygenic radiotherapy.

***Conclusions*:** The non-invasive oxygen enhanced MRI acquisitions proposed here show promising potential to identify those tumors that would generally improve their response to a hypoxia targeted treatment.

Keywords

Glioblastoma multiforme; magnetic resonance imaging; TOLD contrast; BOLD contrast; hypoxia; radiotherapy; oxygen modulation; animal model

1. Introduction

Despite decades of intensive research in different fields, high-grade gliomas (WHO grade III and IV) are still considered incurable, with very unfavorable prognosis [1]. With current medical managements, these malignant brain tumors show mean survival times after diagnosis of 2 to 3 years for anaplastic astrocytoma, and around 15 months for glioblastoma multiforme (GBM) [2]. GBM is, in fact, the most aggressive and lethal intracranial tumor, depicting the highest morbidity and mortality outcomes, notwithstanding its relatively low incidence. Typical treatments of GBM involve surgery followed by chemotherapy and radiation therapy [3], but the 5 years survival prediction remains less than 3% [4]. One of the possible explanations for this lack of treatment success relies in the low availability of oxygen in certain tumor regions [5].

Hypoxia, or low oxygen tension (pO_2), is an important characteristic of advanced solid tumors. It results from an imbalance between oxygen consumption and supply, and has been long recognized as an important determinant of tumor aggressiveness, patient outcome and resistance to different therapeutic interventions including, chemotherapy, radiotherapy and surgical tumor resection [6]. Whereas hypoxia is deleterious to most normal cells causing their death, neoplastic cells can develop adaptive mechanisms to survive under conditions of oxygen limitation [7]. In GBM patients, the hypoxic core, or local hypoxic foci, are highly resistant to different treatments and will induce, most likely, tumor relapse [8]. Low oxygen tension is also linked to treatment resistance at different levels [7]. As a result, several strategies have been previously proposed to alleviate tumor hypoxia and potentiate treatment, including hyperoxic/hyperbaric gas breathing, increasing the ability of blood to carry oxygen (transfusions, administration of erythropoietin), the use of artificial oxygen carriers (perfluorocarbons), hypoxic cell-selective cytotoxins, intensity modulated radiation therapy and gene therapies [7, 9-11]. However, despite promising perspectives in preclinical studies, the new therapeutic interventions delivered only marginal benefits at the clinical level. In particular, the Overgaard meta-analysis [12] concluded that this

lack of efficacy was most likely due to the current inabilities to accurately measure tumor hypoxia *in vivo*, and stratifying adequately those patients that would, most likely, benefit from hypoxia targeted interventions.

Consequently, considerable efforts have been devoted to develop *in vivo* oxygen measurement techniques [9, 13, 14]. But despite the different approaches investigated, there is not currently a technique that fulfills all the desired requirements, and consequently, none of them has been widely adopted in practice [15]. Besides, numerous studies reported high variability of intra- and inter-tumor oxygen tension even within patients with the same tumor type [9, 16, 17], stressing the importance of imaging tumor hypoxia for each patient individually. In the past few years, oxygen enhanced MRI (OE-MRI) has been proposed as an interesting alternative to evaluate the tumoral pO_2 *in vivo*, since it is completely non-invasive, makes use of an endogenous contrast, has adequate temporal and spatial resolution and is easy to implement in the current clinical MRI routines [18]. As a main drawback, it does not provide quantitative pO_2 values, although several studies reported a direct link between OE-MRI derived parameters and changes in pO_2 [19, 20]. OE-MRI takes advantage of two contrast mechanisms directly influenced by oxygenation status: Blood Oxygen Level Dependent (BOLD) and Tissue Oxygen Level Dependent (TOLD). Both BOLD and TOLD measurements, based on changes in signal intensity (SI), coupled with hyperoxic or hyperbaric gas challenge have been tested in preclinical settings [21-23] and in volunteer human patients [24, 25]. Here, we hypothesized that these techniques could provide additionally valuable information to assess tumor response to therapeutic interventions modulating hypoxia levels.

On these grounds, the present study reports on the influence of oxygenation in tumor response to radiotherapy using an orthotopic model of glioblastoma multiforme (GBM) in rats. We explore the use of OE-MRI (BOLD and TOLD) to identify those specific tumors that will benefit from a hypoxia targeted therapy (breathing pure oxygen), designed generally to improve treatment responses.

2. Materials and Methods

The experimental procedures were approved by the highest institutional ethical committee (Community of Madrid) and met the national (R.D. 53/2013) and the European Community guidelines (2010/62/UE) for care and management of experimental animals. Animals were housed in the animal premises of our institution (Reg. No. ES280790000188) and cared by specialized personnel.

2.1 Animal Handling

Male Wistar rats, of body weight (b.w.) 230 ± 20 g, were used. Animals were kept in cages in a controlled room with a 12-h cycle of light and darkness, temperature of 22°C ± 2°C and water and food access *ad libitum*. The study comprised 19 C6 glioma-bearing animals, divided into two groups treated with radiotherapy: 9 rats irradiated under normoxic conditions (air breathing, group 1) and 10 rats irradiated in hyperoxia (100% oxygen breathing, group 2).

2.2 Tumor Implantation

Authenticated rat glioma C6 cells were obtained from the American Type Culture Collection (ATCC number CCL-107, Manassas, VA, USA). Cells were grown in Dulbecco's Modified Eagle´s Medium (DMEM), supplemented with HEPES, 10% fetal bovine serum (FBS) and antibiotics. Briefly, animals were anaesthetized intraperitoneally (i.p.) with a mixture of ketamine/medetomidine (75/0.5 mg/kg) and placed in a stereotaxic holder. Then, 10^5 C6 cells in 10 µL of medium were injected in the right caudate nucleus, through a small craniotomy. After surgery, rats were induced to recover with atipamezole (5 mg/kg) subcutaneously (s.c.) administrated. They also received s.c. meloxicam (0.5 mg/kg) as analgesia during the following 3 days [26].

2.3 MRI Studies

2.3.1 General

In vivo MRI experiments were performed on a Bruker AVANCE III system (Bruker Medical GmbH®, Ettlingen, Germany) using a 7.0-T horizontal superconducting magnet, equipped with a gradient insert (60 mm inner diameter) with a maximum intensity of 360 mT/m and a ^{1}H selective birdcage resonator (38 mm inner diameter). Anesthesia was initiated in an induction box through the inhalation of a mixture containing 3%-4% of isoflurane in air (1 L/min), and maintained during the experiment through a nose mask delivering 1%-1.5% Isoflurane in air (or oxygen). Animals were then placed in a heated probe, which maintained the core body temperature at approximately 37°C. The physiological status of the animals was monitored by a gating system designed for small animals (SA Instruments, Inc., Stony Brook, NY, USA) providing respiratory rate and body temperature through the imaging experiment.

2.3.2 Anatomical Imaging

For assessing the tumor growth, T2-weighted (T2W) spin-echo (SE) images were acquired with a rapid acquisition with relaxation enhancement (RARE) sequence and the following parameters: repetition time (TR) = 3000 ms, echo time (TE) = 60 ms, averages (Av) = 3, RARE factor = 8, acquisition matrix (Mtx) = 256 × 256, in-plane resolution of 136 × 136 µm^2, slice thickness = 1.5 mm and 10 slices in coronal orientation (total acquisition time of 3.36 min). Besides, T2W images were acquired as reference at the end of the complete MRI study.

2.3.3 BOLD Experiments

T2*-weighted (T2*W) images were acquired using a FLASH sequence and the following parameters: TR = 300 ms, TE = 20 ms, Av = 1, Mtx = 128 × 128, in-plane resolution of 234 × 234 µm^2, slice thickness = 1.0 mm and 3 slices in axial orientation (total acquisition time of 38.4 s).

2.3.4 TOLD Experiments

T1-weighted (T1W) FLASH images were acquired using TR = 30.5 ms, TE = 5 ms, Av = 1, and the same geometrical parameters as T2*W images for BOLD studies (total acquisition time of 3.9 s).

2.3.5 Contrast Enhanced (CE) Studies

CE-T1W images were acquired after i.p. administration of 0.2 M Gd-diethylenetriaminepentaacetic acid (Magnevist®, Bayer, Whippany NJ, USA) at a dose of 0.25 mmol/kg b.w. Images were obtained with a SE sequence using TR = 500 ms, TE = 10.6 ms, Av = 2, Mtx = 256 × 256, in-plane resolution of 136 × 136 μm^2, slice thickness = 1.5 mm and 10 slices in coronal orientation (total acquisition time of 3.12 min).

2.3.6 Overall Description of the Experiment Design

Tumor growth follow-up was carried out by acquiring T2W and CE-T1W images, from the day 7-9 after the implantation to the day 38-40, or until the animal experiment reached the endpoint according to ethical procedures. OE-MRI experiments were performed the day before the irradiation as previously described [21]. Briefly, the animals were positioned and anatomical images were acquired in the coronal plane. These images were used to position the axial BOLD and TOLD images so the middle slice goes through the higher section of the tumor. Five alternated BOLD and TOLD studies were performed while the animal was breathing air and these were used as a baseline. Immediately after, the breathing gas was changed to 100% oxygen (group 2, n = 10 animals), or remained as air (group 1, n = 9 animals), and fifteen alternated BOLD and TOLD sequences were acquired. At the end of the experiment, T2W anatomical images with the same geometry as BOLD and TOLD were obtained.

2.4 Radiotherapy

At day 19-21 after C6 cells implantation, animals were irradiated during 11 minutes -either under normoxic (group 1) or hyperoxic conditions (group 2)- by selecting a dose of 10 Gy in a biological irradiator (Shepherd Mark J-30 800 Ci 137Cs). Briefly, the glioma-bearing rats were anesthetized by injecting a mixture of ketamine/medetomidine (75/0.5 mg/kg, i.p. injected) prior to the irradiation. When rats showed proper anesthesia level, they were covered with a home-made lead tube, leaving the head uncovered, thus allowing the radiation reach the tumor. The animals were then placed in the irradiator system over the spinning platform. In order to assure hyperoxia for group 2, once the rat was in the irradiation chamber, the air was displaced by flowing pure oxygen at 5 bar for 15 minutes prior to the irradiation, and this oxygen level was maintained during the whole irradiation procedure.

2.5 Data Analysis

2.5.1 Tumor Volume Analysis

Images were analyzed with Image J software (NIH, USA) [27] and the data obtained treated with Excel software (Microsoft, USA). The volume of the tumors was calculated from anatomical CE-T1W images. In order to normalize tumor response to the therapy, the tumor volume measured the day before the irradiation was chosen as the basal size (value of 0) from which we determined the GBM evolution. Any positive change reflects tumor growth whereas negative change depicts tumor shrink. The relative tumor volume at the end of the experiment (RTVf) was selected for the purposes of analysis.

2.5.2 OE-MRI Analysis

To assess the GBM response to oxygen modulation, we evaluated in each animal the relative changes of TOLD and BOLD signals in the tumor related to the contralateral hemisphere, considered as healthy tissue. These two regions of interest (ROIs), of approximately the same size, were manually selected and delineated in three adjacent slices. Briefly, the signal intensity (SI) of the 5 first images (while the animal was breathing air) from T1W (TOLD contrast) or T2*W acquisitions (BOLD contrast), were averaged in order to obtain the intensity baseline. Normalized changes in SI for each ROI were calculated according to Equation 1:

$$\Delta SI(\%)_i = \frac{SI_i}{\left(\sum_{i=1}^{5} SI_i / 5\right)} \times 100 - 100 \qquad \text{[Eq. 1]}$$

where i is the image number, and SI_i the averaged signal intensity of the ROI in that image.

The TOLD signal in the tumor (T) or in the contralateral hemisphere (C) was calculated as the mean changes of ΔSI during oxygen breathing according to the Equation 2:

$$TOLD_{[T\ or\ C]}(\%) = \frac{\sum_{i=6}^{20} \Delta SI(\%)_i}{15} \qquad \text{[Eq. 2]}$$

Finally, the relative changes of TOLD signal in the tumor, related to the changes in the contralateral hemisphere, were obtained using Equation 3:

$$\Delta TOLD(\%) = \frac{TOLD_T - TOLD_C}{TOLD_T} \times 100 \qquad \text{[Eq. 3]}$$

Equivalent equations 2 and 3 were applied for assessing the BOLD studies.

2.5.3 Statistical Analysis

Statistical analyses were performed using GraphPad Prism 4 software (GraphPad Software, Inc., San Diego, CA, USA). The differences between values were determined by unpaired two tailed Student's t-tests analysis with Welch's correction. Correlation between parameters was assessed using two tailed Pearson correlation coefficients (*R*). In all cases, P values lower than 0.05 were considered to be statistically significant.

3. Results

3.1 Oxygen-Enhanced Magnetic Resonance Imaging

The response to the hyperoxic gas challenge was heterogeneous, but TOLD and BOLD changes within each animal studied were highly consistent. Figure 1 illustrates the obtained results with a representative tumor. The ΔSI maps, measuring signal intensity change in T1W or T2*W images, depict regions with positive (orange) and negative (blue) changes for BOLD (upper panels) and TOLD (lower panels) images during air (Figure 1A & D) and oxygen (Figure 1B & E) breathing, whereas regions of no change are shown in black.

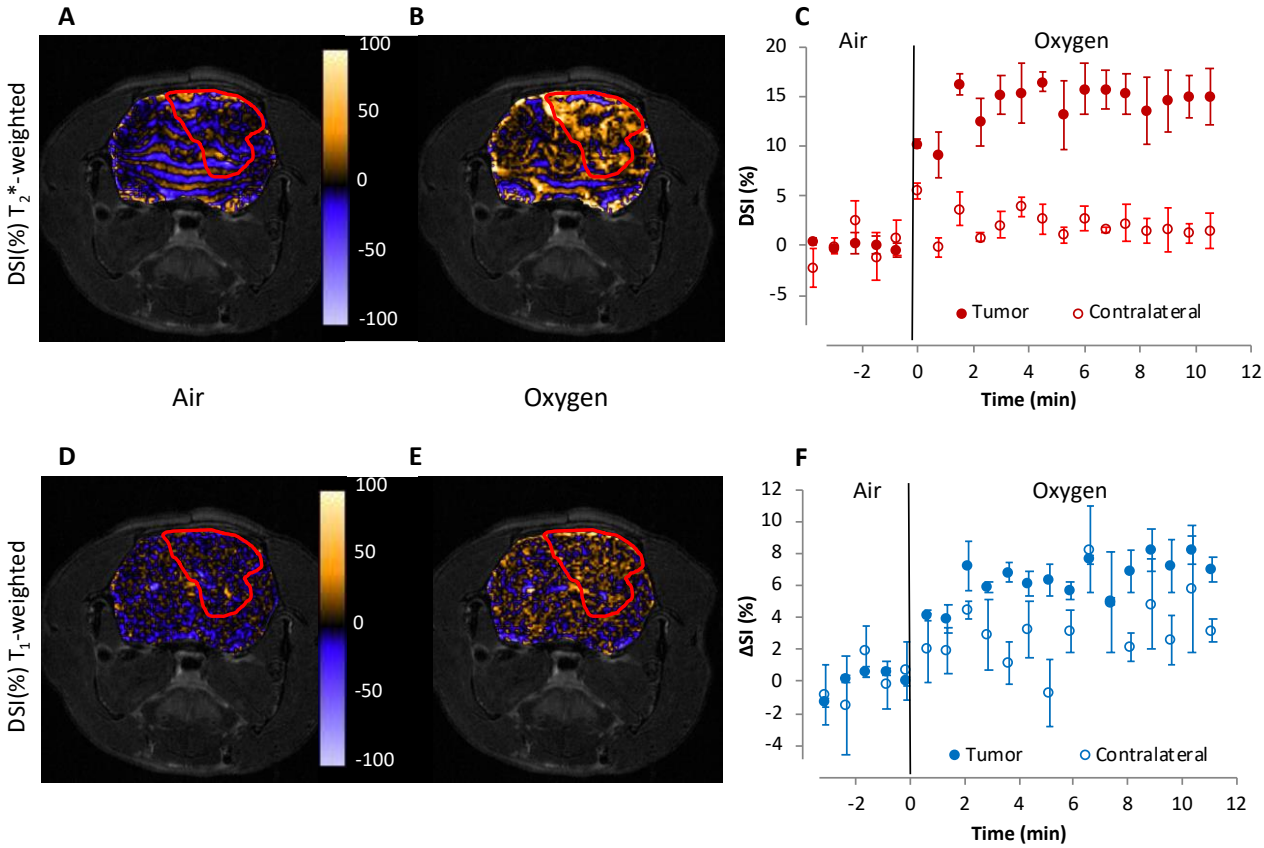

Figure 1 Oxygen-Enhanced MRI. Response maps, as ΔSI, in normalized T2*W (A, B) and T1W (D, E) OE-MRI studies, are overlaid on T2W-SE images of a representative GBM animal. Brain images were acquired while breathing air (A, D) and oxygen (B, E). Tumor is enclosed in a red line. Color-based scale bar shows percentage change in ΔSI. Graphics C and F show the mean BOLD (C) and TOLD (D) responses measured in three adjacent image slices on tumor (filled circles) and contralateral healthy tissue (empty circles). Data are represented as the mean value ± standard error of the mean (SEM).

Mean values were stable during air breathing (Figure 1C for BOLD, and 1F for TOLD), with standard errors ranging from 1 to 4% for BOLD and 1 to 5% for TOLD. When the breathing gas was changed to oxygen, the maps showed an overall increase of the ΔSI values, although areas of negative change become also detectable (Figure 1B and 1E for BOLD and TOLD respectively). BOLD signal in the tumor increased very quickly after oxygen insult (10%), reaching a plateau (15%) at 1.5 min and remaining constant until the end of the experiment. The contralateral healthy hemisphere showed higher variability with time, depicting a cyclic response to oxygen that is attenuated with time until reaching a stable value of around a 2% increase with respect to the baseline. TOLD responses followed a similar pattern but depicted smaller change in ΔSI (7%), as was expected.

In order to evaluate the potential influence of the GBM size in the OE-MRI derived parameters, we investigated whether BOLD and/or TOLD signals in the tumor were driven by its volume the day before the irradiation, when the OE-MRI studies were carried out. Although both BOLD (Figure 2A) and TOLD (Figure 2B) signals showed a tendency to increase with the tumor size, this is not statistically significant (R = 0.336, P = 0.159 for BOLD and R = 0.078, P = 0.75 for TOLD). The same

analysis but using the ΔBOLD (Figure 2C) or ΔTOLD (Figure 2D) instead, yielded similar patterns, not showing significant relationship with tumor size either (R = 0.241, P = 0.321 for ΔBOLD, and R = 0.38, P = 0.11 for ΔTOLD).

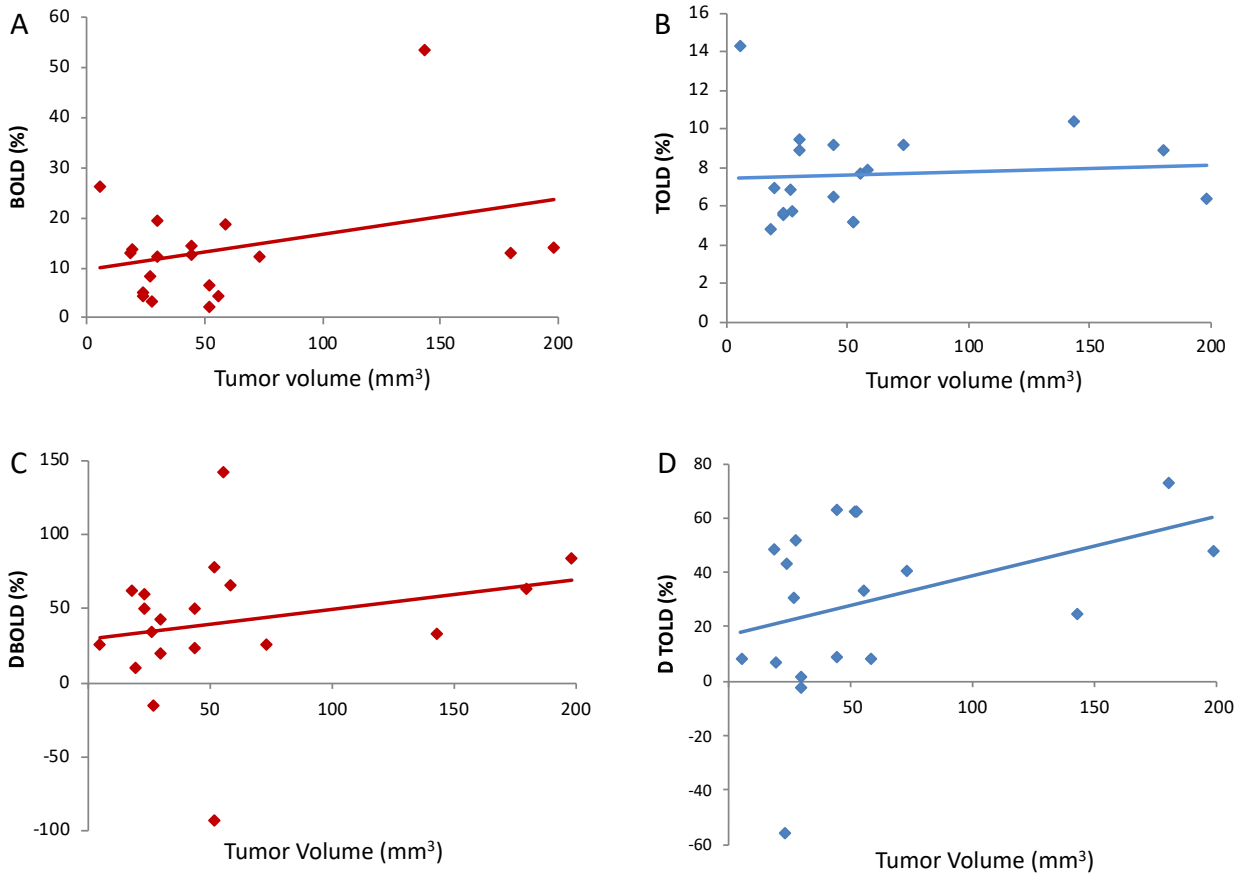

Figure 2 Relationship between OE-MRI data and the tumor volume. Graphics show the correlation analysis of OE-MRI parameters versus the tumor size the day before the irradiation. Panels A and B show the results for BOLD and TOLD measurements in the tumor; C and D present the ΔBOLD and ΔTOLD data, respectively.

We also assessed the possible correlation between BOLD and TOLD changes. As shown in Figure 3A, tumor BOLD and TOLD responses are significantly matched, with a trend of higher TOLD being associated with larger BOLD (R = 0.614, P = 0.005). Nevertheless, this relationship is lost when the changes are tested relative to the contralateral hemisphere (Figure 3B): ΔBOLD vs ΔTOLD (R = -0.035, P = 0.886).

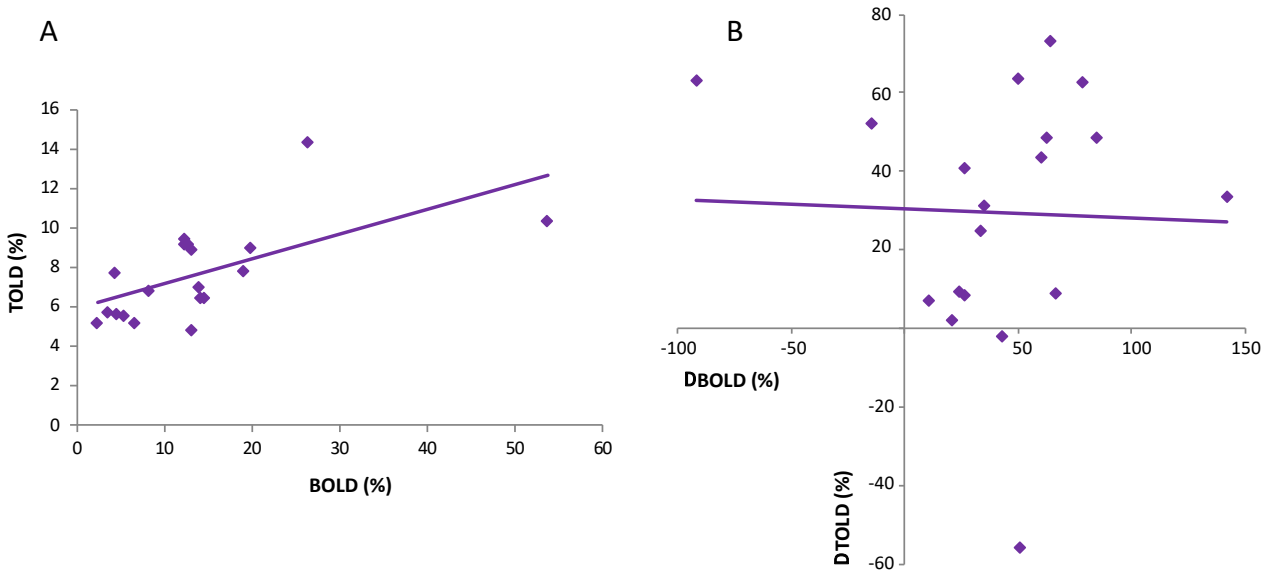

Figure 3 Relationship between BOLD and TOLD responses. Correlation analysis between BOLD and TOLD signals measured in the tumor from OE-MRI studies (A), and between ΔBOLD and ΔTOLD changes from the same experiment (B).

3.2 Radiation Response

Table 1 presents some of the relevant data of the study, including the tumor volume the day before the irradiation, the relative tumor volume at the end of the experiment, and the parameters obtained from the OE-MRI acquisitions.

Taking RTVf as a measure of therapy efficacy, we categorized the tumors in three different groups: animals with a clear positive response in which the glioma volume notably decreased (RTVf < -50%), rats that did not respond to the radiation whose tumor size at least doubled in size (RTVf > 100%), and subjects with an intermediate behavior that could not be clearly included, at least at the end time of the study, in either of the two previous groups (-50% < RTVf < 100%). Under this assumption, in the cohort of animals irradiated in hyperoxic condition, 4 of them were responding (11, 12, 14 and 18), 4 did not respond (10, 13, 16 and 17) and 2 presented an intermediate behavior (15 and 19); while in the group treated under normoxia, only 2 responded (3 and 4), 4 were non-responding (1, 5, 6 and 7) and 3 were identified with the intermediate behavior (2, 8 and 9). Analyzing the data, there were no statistical differences between group 1 (rats 1-9) and 2 (rats 10-19) before irradiation, either in tumor volume or any of the OE-MRI measured parameters. Nevertheless, we found a statistically significant difference in the ΔTOLD values between responding and non-responding animals that were irradiated under pure oxygen breathing ($P = 0.004$). Interestingly, this did not happen for animals irradiated in normoxic conditions, or when BOLD related parameters were tested.

Table 1 GBM tumor characteristics and OE-MRI parameters.

BC	Rat	TV-pre[a]	RTVf[b]	$BOLD_T$[b]	ΔBOLD[b]	$TOLD_T$[b]	ΔTOLD[b]
Group 1 *(Air)*	1	23	356	5.3	61	5.6	43
	2	23	-12	4.5	51	5.7	-56
	3	26	-74	8.3	35	6.8	31
	4	180	-96	13.0	64	8.9	73
	5	44	900	12.7	50	9.2	63
	6	27	395	3.4	-14	5.7	52
	7	44	169	14.5	24	6.5	9
	8	143	10	53.7	34	10.4	25
	9	19	55	13.8	10	7.0	7
Group 2 *(Oxygen)*	10	58	257	19.0	67	7.9	9
	11	52	-75	6.6	78	5.2	63
	10	52	-97	2.3	-92	5.2	63
	13	55	240	4.4	142	7.8	33
	14	199	-90	14.2	85	6.4	48
	15	18	41	13.1	63	4.8	49
	16	29	358	12.2	21	9.5	2
	17	29	451	19.7	43	9.0	-2
	18	73	-85	12.3	26	9.2	41
	19	5	55	26.3	27	14.4	8

BC: Breathing condition
TV-pre: Tumor volume the day before the irradiation (pre-treatment)
a: Data are presented as mm^3
RTVf: Relative tumor volume at the end of the experiment
b: Data are presented as percentage (%)
T: Tumor

Figure 4 shows anatomical CE-T1W acquisitions of two representative animals at several time points before and after the irradiation. Images A-D correspond to a non-responding animal treated under normoxic conditions whereas images E-H represent a responding animal irradiated under oxygen breathing.

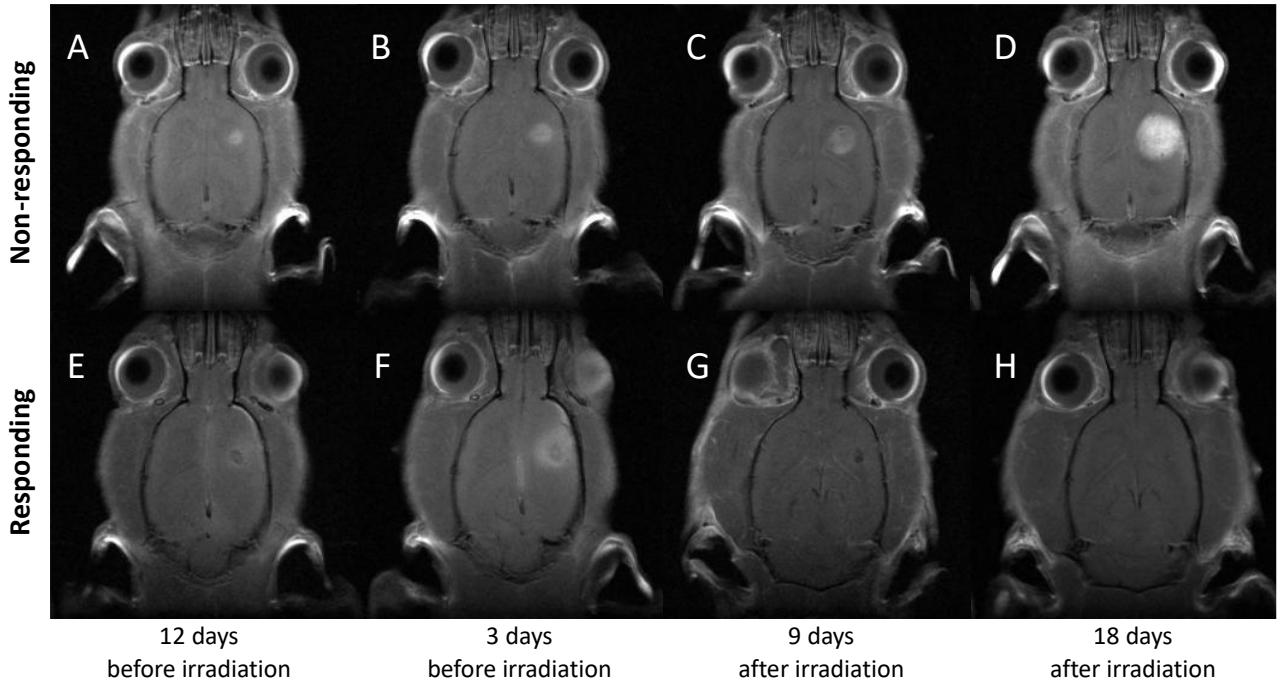

Figure 4 Representative CW-T1W MRI of tumor evolution, before (12 and 3 days) and after (9 and 18 days) the irradiation. Top images correspond to a GBM bearing animal that did not respond to irradiation under normoxic conditions (A-D); while the bottom ones (E-H), correspond to an animal that did respond to irradiation in hyperoxia.

Finally, we pursued to evaluate the correlations between tumor response to treatment, as measured by the RTVf, and OE-MRI parameters. When ΔBOLD response was tested (Figure 5A), no correlation was found for any of the two groups (R = -0.044, P = 0.91 for air and R =0.24, P = 0.5 for oxygen breathing animals respectively). This was also the case for ΔTOLD response in animals irradiated during air breathing (Figure 5B, R =0.401, P = 0.28).

Nevertheless, a strong negative correlation was found between ΔTOLD and RTVf for animals breathing oxygen during irradiation, with R = -0.846 and P = 0.002. Within the cohort of tumors irradiated during oxygen breathing, all the responding animals present a ΔTOLD > 40%, whereas all the non-responding in the same group showed a ΔTOLD < 40%. Those tumors with an intermediated behavior showed mixed values for ΔTOLD (48 and 8%) despite showing similar responses to irradiation (RTVf = 41 and 55 % respectively, corresponding to tumors 15 and 19 in Table 1).

As we found animals responding to irradiation in both normoxic and hyperoxic groups, we evaluated whether OE-MRI could be a good predictor of the tumor response to radiotherapy irrespective of the breathing conditions during the treatment. If we put all the tumors together, we find no correlation between any of the OE-MRI parameters (BOLD, TOLD, ΔBOLD, ΔTOLD) and the relative volume at the end of the study (data not shown).

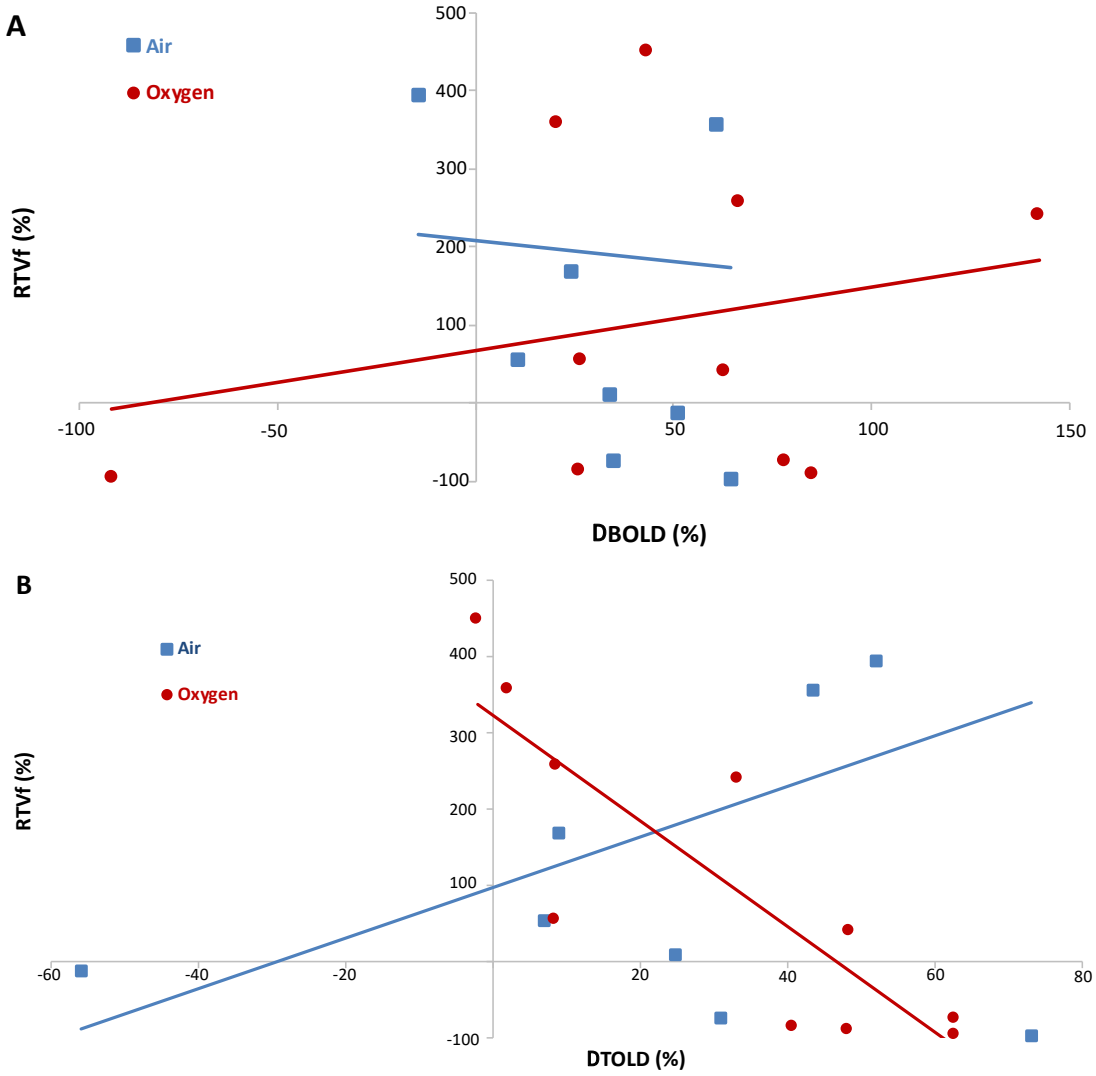

Figure 5 Correlations between OE-MRI parameters and the relative tumor volume at the end of the experiment. A: No correlation was found when ΔBOLD was tested, either for tumors irradiated under normoxia (blue points) or hyperoxia (red points). B: A strong correlation was observed for ΔTOLD (%) in animals that inhaled pure oxygen during irradiation (R = -0.846, P = 0.002), but not in those treated under air breathing (R = 0.401, P = 0.28).

4. Discussion

It is widely accepted that tumor hypoxia plays a central role in therapy failure and poor patient outcome [15, 28, 29]. This is especially important in radiotherapy, with several studies linking its success to tumor oxygenation [30, 31]. Consequently, numerous strategies have been developed over the years to modulate tumor pO_2 to improve therapy efficacy. Among them, hyperoxic or hyperbaric gas breathing [7] have been a very popular choice due to its easy application [22], low cost and minimal impact in patient health [32]. Several studies have proved the suitability of this strategy with different tumor types, including prostate [33], liver [34], breast [35], cervix [36, 37] and brain [25, 38]. However, despite the success achieved in pre-clinical settings, the expectations became much attenuated when translated to the clinic [7, 39]. One of the possible reasons for this

circumstance, is the lack of a proper method to identify those patients that would benefit from a hypoxia directed intervention [12, 13, 15], as neither, the tumor oxygenation nor the response to hypoxia directed therapies could be inferred from histopathological or conventional imaging studies. This situation emphasized the need to measure tumor pO_2 and/or response to hypoxia directed therapies on a patient by patient personalized manner.

Oxygen enhanced MRI provides a convenient methodology to measure tumor response to hypoxia targeted interventions, as it is sensitive to changes in oxygenation, does not require an external contrast agent nor ionizing radiation, it is non-invasive and uses currently available MRI technology. All these circumstances, promise to facilitate translation to the clinical environment and its combination with additional MRI techniques yielding multiparametric information. OE-MRI is based on the different magnetic properties of hemoglobin in vessels, and molecular oxygen in tissues. Hemoglobin is diamagnetic in its oxygenated form whereas paramagnetic when unbound to molecular oxygen. The ratio oxy- to deoxy-hemoglobin influences the apparent transverse relaxation rate, which is the basis for the BOLD contrast. BOLD has been used in many functional MRI studies as a surrogated marker of neuronal activation [9] and more recently, to investigate the response of tumors to hyperoxic gas challenges [19, 40]. Several studies have recently taken advantage of the weak paramagnetic properties of molecular oxygen in aqueous solvents, because of its two unpaired electrons. Due to this circumstance, dissolved molecular oxygen will decrease the longitudinal relaxation time of tissue water. Unlike with hemoglobin, this relationship is nearly linear at physiological conditions [41], and this is the basis of TOLD contrast [21]. Several studies have shown the feasibility of this approach to assess changes in tumor oxygenation coupled with the modulation breathing atmospheres [21, 42].

On these grounds, the present study aimed to assess the potential prognostic utility of OE-MRI as an *in vivo* and non-invasive imaging strategy to predict the tumor radiotherapy response in hyperoxic conditions. A GBM model generated by C6 glioma cell intracranial injection was selected due to its favorable characteristics: it is hypoxic ($pO_2 \approx$ 12-14 mm Hg) but still responsive to pO_2 modulation by hyperoxic gas breathing [43]; reacts to radiation; presents a high grade of heterogeneity [44], which more accurately reflects the clinical situation; and grows orthotopically in a non-homogenous pattern between individuals, increasing malignancy as it develops [45]. We found that our model presents a high-grade of variability in response to radiotherapy, irrespective of the tumor size or the conditions used during treatment (Table 1, Figure 4 & 5). To improve tumor oxygenation, we employed pure oxygen breathing. Finally, we selected radiotherapy since its outcome can be improved by increasing tumor oxygenation [20, 46].

The goal of any applied therapy is to achieve the maximum treatment response in the affected tissue while minimizing damage to the surrounding normal tissue. In order to monitor this, we focused here on those parameters that best depict the difference in oxygenation status between tumor and contralateral brain, instead of relying merely on the glioma response. On these grounds, we chose ΔBOLD or ΔTOLD as our reference parameters, since they reflect the above-mentioned difference between cancerous and healthy tissues. ΔSI maps during air breathing (Figure 1 A & D) showed fluctuation in SI during baseline conditions both in healthy and in tumor tissue. This fact reflects the normal tissue fluctuation in oxygenation status, and it is the basis for resting state functional MRI [47]. Besides, it is well stablished that tumor volume is not a good predictor of either tumor oxygenation or treatment outcome [48], and it has little or no influence on OE-MRI studies [41]. Since, to the best of our knowledge, no previous information was available on OE-

MRI in orthotopic C6 GBM model, we investigated the influence of tumor size on BOLD and TOLD responses (Figure 2). Although there is a tendency towards higher BOLD and TOLD responses with higher tumor volume, these are not statistically significant. We also confirmed that tumor size before the treatment is not a good predictor of the therapy outcome, as measured by the RTVf. It does not matter whether we consider all the tumors together, we separated them based on the irradiation conditions, or in its responsiveness, there was not any statistically significant correlation between these two parameters. Nevertheless, we found that ΔTOLD is a parameter that is highly correlated (R = -0.85, P = 0.002) with the RTVf in the cohort of animals irradiated under hyperoxic conditions (Figure 5B). Furthermore, ΔTOLD was also significantly different for responding vs non-responding tumors treated under oxygen breathing (P = 0.004). No correlation, or significant difference, was found in the analysis of tumors that were irradiated while animals were breathing air.

These results are consistent with those obtained in previous studies using a prostate tumor model (AT1) implanted in the flank. Tumor TOLD response was closely related to tumor growth delay following single [20] or hypofractionated [22] radiotherapy. Sheng Li et al found that T2* has a prognostic value in detecting those patients with cervical squamous carcinoma who have a higher probability of responding positively to chemotherapy [49]. Similar results were reported when assessing BOLD as a predictor of the therapeutic response to chemoradiotherapy in cervical cancer [50]. Jiang et al. [51] also found that large BOLD response correlated with better chemotherapy outcome in patients with locally advanced breast cancer.

There are several limitations to our study. First, due to the high grade of heterogeneity in the tumor response to treatment, the number of animals irradiated in oxygen breathing conditions showing improvement (four) or no responsiveness (four) is too small to establish a strong predictive value. Furthermore, we found that animals depicting intermediate behavior (two) presented mixed responses in ΔTOLD. Thus, more subjects should be added to further assess the predictive potential of this parameter. Second, the therapy was applied at a single time point. It would be also interesting to investigate whether OE-MRI has predictive value at different time points during GBM development. Future studies will consider these and other factors, such as using other parameters to measure therapy success or combining the information provided by OE-MRI with multiparametric MRI studies that can be also be used as surrogate markers of the tumor status.

5. Conclusions

In summary, OE-MRI studies show a promising potential to identify those tumors that would benefit from oxygen breathing during irradiation and, more generally, from any hypoxia targeted therapy. It also reveals profound consequences of the modulation of oxygen content in the breathing gas mixture, for the outcome of therapy. It also reveals that the tumor response cannot be readily predicted from physiopathological parameters or convectional imaging studies.

Author Contributions

All authors contributed equally to the conception and design of the work, data collection, data analysis and interpretation, drafting the article, critical revision of the article and final approval of the version to be published.

Funding

This work was supported by grants from the Ministry of Economy, Industry and Competitiveness (SAF2017-83043-R), and by the Program MULTITARGET&VIEW-CM from the Community of Madrid (S-BIO-0170-2006), involving contributions from FEDER and FSE funds.

Competing Interests

The authors have declared that no competing interests exist.

References

1. Louis DN, Perry A, Reifenberger G, von Deimling A, Figarella-Branger D, Cavenee WK, et al. The 2016 world health organization classification of tumors of the central nervous system: A summary. Acta Neuropathol. 2016; 131: 803-820.
2. Johnson DR, Galanis E. Medical management of high-grade astrocytoma: Current and emerging therapies. Semin Oncol. 2014; 41: 511-522.
3. Davis ME. Glioblastoma: Overview of disease and treatment. Clin J Oncol Nurs. 2016; 20: S2-8.
4. McGuire S. World cancer report 2014. Geneva, switzerland: World health organization, international agency for research on cancer, who press, 2015. Adv Nutr. 2016; 7: 418-419.
5. Hockel M, Vaupel P. Tumor hypoxia: Definitions and current clinical, biologic, and molecular aspects. J Natl Cancer Inst. 2001; 93: 266-276.
6. Muz B, de la Puente P, Azab F, Azab AK. The role of hypoxia in cancer progression, angiogenesis, metastasis, and resistance to therapy. Hypoxia (Auckl). 2015; 3: 83-92.
7. Stepien K, Ostrowski RP, Matyja E. Hyperbaric oxygen as an adjunctive therapy in treatment of malignancies, including brain tumours. Med Oncol. 2016; 33: 101.
8. Monteiro AR, Hill R, Pilkington GJ, Madureira PA. The role of hypoxia in glioblastoma invasion. Cells. 2017; 6.
9. Pacheco-Torres J, Lopez-Larrubia P, Ballesteros P, Cerdan S. Imaging tumor hypoxia by magnetic resonance methods. NMR in biomedicine. 2011; 24: 1-16.
10. Wigerup C, Pahlman S, Bexell D. Therapeutic targeting of hypoxia and hypoxia-inducible factors in cancer. Pharmacol Ther. 2016; 164: 152-169.
11. Feldman LA, Fabre MS, Grasso C, Reid D, Broaddus WC, Lanza GM, et al. Perfluorocarbon emulsions radiosensitise brain tumors in carbogen breathing mice with orthotopic gl261 gliomas. PLoS One. 2017; 12: e0184250.
12. Overgaard J. Hypoxic radiosensitization: Adored and ignored. J Clin Oncol. 2007; 25: 4066-4074.
13. Horsman MR, Mortensen LS, Petersen JB, Busk M, Overgaard J. Imaging hypoxia to improve radiotherapy outcome. Nat Rev Clin Oncol. 2012; 9: 674-687.
14. Mirabello V, Cortezon-Tamarit F, Pascu SI. Oxygen sensing, hypoxia tracing and in vivo imaging with functional metalloprobes for the early detection of non-communicable diseases. Front Chem. 2018; 6: 27.
15. Tatum JL, Kelloff GJ, Gillies RJ, Arbeit JM, Brown JM, Chao KS, et al. Hypoxia: Importance in tumor biology, noninvasive measurement by imaging, and value of its measurement in the management of cancer therapy. Int J Radiat Biol. 2006; 82: 699-757.

16. Brizel DM, Rosner GL, Prosnitz LR, Dewhirst MW. Patterns and variability of tumor oxygenation in human soft tissue sarcomas, cervical carcinomas, and lymph node metastases. Int J Radiat Oncol Biol Phys. 1995; 32: 1121-1125.
17. Brizel DM, Dodge RK, Clough RW, Dewhirst MW. Oxygenation of head and neck cancer: Changes during radiotherapy and impact on treatment outcome. Radiother Oncol. 1999; 53: 113-117.
18. Baker LC, Boult JK, Jamin Y, Gilmour LD, Walker-Samuel S, Burrell JS, et al. Evaluation and immunohistochemical qualification of carbogen-induced deltar(2) as a noninvasive imaging biomarker of improved tumor oxygenation. Int J Radiat Oncol Biol Phys. 2013; 87: 160-167.
19. Zhao D, Jiang L, Hahn EW, Mason RP. Comparison of 1h blood oxygen level-dependent (bold) and 19f mri to investigate tumor oxygenation. Magn Reson Med. 2009; 62: 357-364.
20. Hallac RR, Zhou H, Pidikiti R, Song K, Stojadinovic S, Zhao D, et al. Correlations of noninvasive bold and told mri with po2 and relevance to tumor radiation response. Magn Reson Med. 2014; 71: 1863-1873.
21. Zhao D, Pacheco-Torres J, Hallac RR, White D, Peschke P, Cerdan S, et al. Dynamic oxygen challenge evaluated by nmr t1 and t2*--insights into tumor oxygenation. NMR in biomedicine. 2015; 28: 937-947.
22. White DA, Zhang Z, Li L, Gerberich J, Stojadinovic S, Peschke P, et al. Developing oxygen-enhanced magnetic resonance imaging as a prognostic biomarker of radiation response. Cancer Lett. 2016; 380: 69-77.
23. Winter JD, Akens MK, Cheng HL. Quantitative mri assessment of vx2 tumour oxygenation changes in response to hyperoxia and hypercapnia. Phys Med Biol. 2011; 56: 1225-1242.
24. Ding Y, Mason RP, McColl RW, Yuan Q, Hallac RR, Sims RD, et al. Simultaneous measurement of tissue oxygen level-dependent (told) and blood oxygenation level-dependent (bold) effects in abdominal tissue oxygenation level studies. J Magn Reson Imaging. 2013; 38: 1230-1236.
25. Remmele S, Sprinkart AM, Muller A, Traber F, von Lehe M, Gieseke J, et al. Dynamic and simultaneous mr measurement of r1 and r2* changes during respiratory challenges for the assessment of blood and tissue oxygenation. Magn Reson Med. 2013; 70: 136-146.
26. Perez-Carro R, Cauli O, Lopez-Larrubia P. Multiparametric magnetic resonance in the assessment of the gender differences in a high-grade glioma rat model. EJNMMI Res. 2014; 4: 44.
27. Schneider CA, Rasband WS, Eliceiri KW. Nih image to imagej: 25 years of image analysis. Nat Methods. 2012; 9: 671-675.
28. Mupparaju S, Hou H, Lariviere JP, Swartz H, Jounaidi Y, Khan N. Repeated tumor oximetry to identify therapeutic window during metronomic cyclophosphamide treatment of 9l gliomas. Oncol Rep. 2011; 26: 281-286.
29. Colliez F, Gallez B, Jordan BF. Assessing tumor oxygenation for predicting outcome in radiation oncology: A review of studies correlating tumor hypoxic status and outcome in the preclinical and clinical settings. Front Oncol. 2017; 7: 10.
30. Hou H, Lariviere JP, Demidenko E, Gladstone D, Swartz H, Khan N. Repeated tumor po(2) measurements by multi-site epr oximetry as a prognostic marker for enhanced therapeutic efficacy of fractionated radiotherapy. Radiother Oncol. 2009; 91: 126-131.

31. Hou H, Dong R, Lariviere JP, Mupparaju SP, Swartz HM, Khan N. Synergistic combination of hyperoxygenation and radiotherapy by repeated assessments of tumor po2 with epr oximetry. J Radiat Res. 2011; 52: 568-574.
32. Moen I, Stuhr LE. Hyperbaric oxygen therapy and cancer--a review. Target Oncol. 2012; 7: 233-242.
33. Alonzi R, Padhani AR, Maxwell RJ, Taylor NJ, Stirling JJ, Wilson JI, et al. Carbogen breathing increases prostate cancer oxygenation: A translational mri study in murine xenografts and humans. Br J Cancer. 2009; 100: 644-648.
34. Patterson AJ, Priest AN, Bowden DJ, Wallace TE, Patterson I, Graves MJ, et al. Quantitative bold imaging at 3t: Temporal changes in hepatocellular carcinoma and fibrosis following oxygen challenge. J Magn Reson Imaging. 2016; 44: 739-744.
35. Rakow-Penner R, Daniel B, Glover GH. Detecting blood oxygen level-dependent (bold) contrast in the breast. J Magn Reson Imaging. 2010; 32: 120-129.
36. Hallac RR, Ding Y, Yuan Q, McColl RW, Lea J, Sims RD, et al. Oxygenation in cervical cancer and normal uterine cervix assessed using blood oxygenation level-dependent (bold) mri at 3t. NMR in biomedicine. 2012; 25: 1321-1330.
37. O'Connor JP, Naish JH, Parker GJ, Waterton JC, Watson Y, Jayson GC, et al. Preliminary study of oxygen-enhanced longitudinal relaxation in mri: A potential novel biomarker of oxygenation changes in solid tumors. Int J Radiat Oncol Biol Phys. 2009; 75: 1209-1215.
38. Linnik IV, Scott ML, Holliday KF, Woodhouse N, Waterton JC, O'Connor JP, et al. Noninvasive tumor hypoxia measurement using magnetic resonance imaging in murine u87 glioma xenografts and in patients with glioblastoma. Magn Reson Med. 2014; 71: 1854-1862.
39. Bennett MH, Feldmeier J, Smee R, Milross C. Hyperbaric oxygenation for tumour sensitisation to radiotherapy. Cochrane Database Syst Rev. 2018; 4: CD005007.
40. Zhang LJ, Zhang Z, Xu J, Jin N, Luo S, Larson AC, et al. Carbogen gas-challenge blood oxygen level-dependent magnetic resonance imaging in hepatocellular carcinoma: Initial results. Oncol Lett. 2015; 10: 2009-2014.
41. Beeman SC, Shui YB, Perez-Torres CJ, Engelbach JA, Ackerman JJ, Garbow JR. O2 -sensitive mri distinguishes brain tumor versus radiation necrosis in murine models. Magn Reson Med. 2016; 75: 2442-2447.
42. Matsumoto K, Bernardo M, Subramanian S, Choyke P, Mitchell JB, Krishna MC, et al. Mr assessment of changes of tumor in response to hyperbaric oxygen treatment. Magn Reson Med. 2006; 56: 240-246.
43. Khan N, Li H, Hou H, Lariviere JP, Gladstone DJ, Demidenko E, et al. Tissue po2 of orthotopic 9l and c6 gliomas and tumor-specific response to radiotherapy and hyperoxygenation. Int J Radiat Oncol Biol Phys. 2009; 73: 878-885.
44. Kondziolka D, Lunsford LD, Claassen D, Pandalai S, Maitz AH, Flickinger JC. Radiobiology of radiosurgery: Part ii. The rat c6 glioma model. Neurosurgery. 1992; 31: 280-287; discussion 287-288.
45. Biasibetti E, Valazza A, Capucchio MT, Annovazzi L, Battaglia L, Chirio D, et al. Comparison of allogeneic and syngeneic rat glioma models by using mri and histopathologic evaluation. Comp Med. 2017; 67: 147-156.

46. Khan N, Mupparaju S, Hekmatyar SK, Hou H, Lariviere JP, Demidenko E, et al. Effect of hyperoxygenation on tissue po2 and its effect on radiotherapeutic efficacy of orthotopic f98 gliomas. Int J Radiat Oncol Biol Phys. 2010; 78: 1193-1200.
47. Lee MH, Smyser CD, Shimony JS. Resting-state fmri: A review of methods and clinical applications. AJNR Am J Neuroradiol. 2013; 34: 1866-1872.
48. Vaupel P, Thews O, Hoeckel M. Treatment resistance of solid tumors: Role of hypoxia and anemia. Med Oncol. 2001; 18: 243-259.
49. Li XS, Fan HX, Fang H, Song YL, Zhou CW. Value of r2* obtained from t2*-weighted imaging in predicting the prognosis of advanced cervical squamous carcinoma treated with concurrent chemoradiotherapy. J Magn Reson Imaging. 2015; 42: 681-688.
50. Kim CK, Park SY, Park BK, Park W, Huh SJ. Blood oxygenation level-dependent mr imaging as a predictor of therapeutic response to concurrent chemoradiotherapy in cervical cancer: A preliminary experience. Eur Radiol. 2014; 24: 1514-1520.
51. Jiang L, Weatherall PT, McColl RW, Tripathy D, Mason RP. Blood oxygenation level-dependent (bold) contrast magnetic resonance imaging (mri) for prediction of breast cancer chemotherapy response: A pilot study. J Magn Reson Imaging. 2013; 37: 1083-1092.